Available online at www.sciencedirect.com

ScienceDirect

Ceramics International 40 (2014) 3969–3973

CERAMICS INTERNATIONAL

www.elsevier.com/locate/ceramint

MCM-41 supported CuO/Bi_2O_3 nanoparticles as potential catalyst for 1,4-butynediol synthesis

Guihua Yang[a,b], Yuebing Xu[b], Xintai Su[b], Yahong Xie[b], Chao Yang[b], Zejuan Dong[b], Jide Wang[b,*]

[a]School of Science, Xi'an Jiaotong University, Xi'an 710049, China

[b]Ministry Key Laboratory of Oil & Gas Fine Chemicals, College of Chemistry and Chemical Engineering, Xinjiang University, Urumqi 830046, China

Received 29 June 2013; received in revised form 18 July 2013; accepted 8 August 2013

Available online 16 August 2013

Abstract

CuO/Bi_2O_3 (CuO/Bi_2O_3/MCM-41) nanoparticles supported on MCM-41 were synthesized by a facile impregnation method. The products were characterized by nitrogen adsorption/desorption, X-ray diffraction (XRD), H_2 temperature programmed reduction (H_2-TPR) and scanning electron microscopy (SEM). XRD patterns indicated the presence of crystalline CuO and Bi_2O_3 phase for CuO/Bi_2O_3/MCM-41 catalyst. TPR results revealed CuO nanoparticles were dispersed well on MCM-41. SEM results showed that the nanoparticles were located on the MCM-41. The activity of the catalysts towards ethynylation of formaldehyde for 1,4-butynediol synthesis was evaluated at atmospheric pressure. Compared with unsupported CuO/Bi_2O_3 and commercial Cu/Bi-based catalyst, CuO/Bi_2O_3/MCM-41 catalyst showed maximum conversion (51%) and selectivity (94%) towards 1,4-butynediol. The results show that CuO/Bi_2O_3 catalysts supported on MCM-41 have potential for 1,4-butynediol synthesis in industrial application.

Keywords: A. Powders: chemical preparation; B. Porosity; D. Transition metal oxides; E. Structural applications

1. Introduction

1,4-Butynediol (B_3D) is a valuable intermediate to synthesize 1,4-butanediol (BDO) [1–3]. BDO is predominately used as a feedstock in production of polyurethanes, polybutylene terephthalate (PBT), gamma-butyrolactone and tetrahydrofuran (THF) [4,5]. Due to its commercial importance, B_3D synthesis has been received much attention recently [6,7]. B_3D is mainly synthesized by ethynylation reaction of formaldehyde over Cu/Bi-based catalysts [8,9]. In these Cu/Bi-based catalysts, copper oxide is the main active component and bismuth oxide is usually added into the catalysts for effectively restraining the formation of cuprene and improving CuO crystallite dispersion [10].

Traditionally, unsupported or supported Cu/Bi-based catalysts [11–16] are employed for the ethynylation reaction of formaldehyde. The unsupported Cu/Bi catalysts, such as man-made malachite [12], nano Cu/Bi catalysts [13], often have high activity. However, they are poor abrasion resistance and difficult to be separated from the reaction system [17]. To solve the above problems, Cu/Bi catalysts were loaded on different carriers including SiO_2–MgO [14], HZSM-5 molecular sieve [15], kaolin [16], etc. Among them, SiO_2–MgO [14] has been loaded Cu/Bi components by a co-precipitation method, and a high catalytic activity towards 1,4-butynediol was obtained due to the high dispersion of CuO and Bi_2O_3. Yang [15] has reported that Cu/Bi catalysts supported on HZSM-5 molecular sieve was prepared by impregnation method, and investigated its activity under different ethynylation reaction condition. Luo [16] has developed Cu/Bi catalysts supported on kaolin by deposition–precipitation method, and found they also exhibited good performance in ethynylation reaction of formaldehyde. Therefore, in spite of some success, it is desirable to explore other carrier loaded with Cu/Bi components for 1,4-butynediol synthesis.

It is well known that MCM-41 molecular sieve with ordered pore structures and large surface area has been widely used as a carrier in many catalytic reactions [18–20]. Additionally, MCM-41, containing a large number of silanol groups at the surface of the channels, may make CuO diffuse easily [21]. And CuO can be loaded on inner or outer surface by reaction with silanol groups, as a result, the amounts of Cu loading and

---

*Corresponding author. Tel.: +86 991 8581018; fax: +86 991 8582807.
E-mail address: awangjd@sina.cn (J. Wang).

0272-8842/$ - see front matter © 2013 Elsevier Ltd and Techna Group S.r.l. All rights reserved.
http://dx.doi.org/10.1016/j.ceramint.2013.08.044

losing may be decreased and there is little residual Cu in products [22]. Hereby, we report Cu/Bi catalysts supported on MCM-41 molecular sieve prepared by a facile impregnation method. The as-prepared CuO/Bi_2O_3/MCM-41 catalysts have shown excellent performance in ethynylation reaction for 1,4-butynediol synthesis. Furthermore, the activity of the CuO/Bi_2O_3/MCM-41 catalysts was also compared with that of an unsupported CuO/Bi_2O_3 catalyst and a commercial Cu/Bi-based catalyst. The results showed that the CuO/Bi_2O_3/MCM-41 catalysts can be used as high effective catalyst for the synthesis of 1,4-butynediol.

2. Experimental

2.1. Catalyst preparation

The CuO/Bi_2O_3/MCM-41 catalyst was prepared by an impregnation technique [15]. A commercially available, pure-silica MCM-41 zeolite (Catalyst Plant of Nankai University) was first impregnated with an aqueous mixture of Cu $(NO_3)_2$, Bi $(NO_3)_3$ and concentrated HNO_3 at room temperature for 10 h. The concentrated HNO_3 was to avoid the precipitation of Bi^{3+} ion. After the impregnation, followed by dehydration in a vacuum rotary, the catalyst was dried at 120 °C overnight and finally calcined in air at 480 °C for 6 h.

The CuO/Bi_2O_3 catalyst was prepared by a co-precipitation method [11]. Na_2CO_3 solution was quantitatively added to an aqueous solution of Cu $(NO_3)_2$ and Bi $(NO_3)_3$ and the pH was adjusted to 7.5. The mixture was stirred for 30 min and heated to 45 °C. The suspension was then aged for 2 h at room temperature; the resulting precipitate was washed repeatedly with hot deionized water till the filtrate was neutral, dried at 120 °C overnight and calcined in air at 450 °C for 5.5 h.

The commercial Cu/Bi-based catalyst was obtained from a chemical company in China denoted as MK.

2.2. Catalyst characterization

The powder X-ray diffraction (XRD) patterns of samples were collected on a DX-2000 X-ray diffractometer (Dandong Instruments, China) using Cu Kα radiation ($\lambda = 0.15418$ nm) and the scanning rate was set at 1.2°/min over a 2 theta range of 2～80°. N_2 adsorption and desorption isotherms of the samples were measured in a BET apparatus (JW-BK analyzer, China) at −196 °C to evaluate their surface areas and pore volumes. The tested samples were degassed at 105 °C for 2 h under vacuum before their measurements. H_2 temperature programmed reduction (H_2-TPR) was performed to evaluate the reduction properties of the as-prepared materials. The measurements were conducted in an auto-controlled flow reactor system with a thermal conductivity detector (TP-5080, China). 50 mg of a sample was used for each measurement. The sample was first treated in a N_2 stream at 500 °C for 1 h, cooled down to 50 °C and then heated in a 10% H_2/N_2 stream to 500 °C at a heating rate of 15 °C/min to obtain the H_2-TPR pattern. The morphology of the samples was observed on a LEO1430VP scan electron microscopy (SEM). The Cu^{2+} and Bi^{3+} contents in all prepared catalysts were determined using the method of atomic absorption spectroscopy on a Hitachi Z-2000.

2.3. Catalyst evaluation

All catalytic tests of ethynylation of formaldehyde with acetylene were carried out in a three-neck flask connected with reflux condenser, thermocouple and a three-way valve at atmospheric pressure. A certain amount of catalysts and approximately 20 g formaldehyde (20 wt%) water solution were together added in the flask placed in an oil bath with electromagnetic stirring, followed by loading 0.1 mol/L Na_2CO_3–$NaHCO_3$ buffer solution for adjusting the pH value of the solution to 7.5. Before the reaction, a flow of pure N_2 was introduced into the flask through a three-way valve to purge O_2 inside the flask for the experiment safety, and then C_2H_2 was also introduced into the flask after N_2 stream was stopped. After that, the solution with the catalyst was stirred continually and heated to 75 °C and then kept in the continuous C_2H_2 stream for 4 h. During the treatment, the catalyst was activated and its color turned to brick red. Next, the solution was heated to 90 °C to start the ethynylation of formaldehyde under the continuous flow of C_2H_2. Several hours later, the catalytic reaction was stopped by introducing a N_2 stream and closing the C_2H_2 stream and the solution was cooled down to room temperature.

The used catalyst was filtered and dried under vacuum. In the filtrate, the formaldehyde content was determined by titration with sodium sulfite to obtain the conversion of formaldehyde while the 1,4-butynediol content was analyzed using gas chromatography (Shimadzu, GC-14B) equipped a FID detector and a RTX-5 capillary column using a 1,4-butanediol-added internal standard method. The selectivity to1,4-butynediol was obtained by dividing the yield of 1,4-butynediol by the conversion of formaldehyde.

3. Results and discussion

3.1. Textural properties of the samples

The textural properties of the tested samples are listed in Table 1. The unsupported CuO/Bi_2O_3 catalyst loaded with 69.4% Cu and 7.9% Bi, and commercial MK catalyst loaded with 35.6% Cu and 4.0% Bi, possessed the lower surface areas and pore volumes due to their nonporous structures. The blank MCM-41 zeolite possessed large surface area and pore volume of 1095 m^2/g and 1.24 cm^3/g, respectively, while its surface area and pore volume decreased to 709 m^2/g and 0.76 cm^3/g after loaded with 23% Cu and 6% Bi. This suggested that the impregnated ions, especially the Cu ions might, have dispersed into the channels of the MCM-41 zeolite crystals or near their openings. The mean pore diameter in the CuO/Bi_2O_3/MCM-41 was only slightly different from the blank MCM-41, indicating that the mesopores in the MCM-41 were not destroyed after loading the metal oxides. The mean pore diameter in the unsupported CuO/Bi_2O_3 catalyst or MK catalyst might be associated with pores existing between the particles. Compared

Table 1
Textural property of MCM-41 and catalyst samples.

Sample	Cu content /wt%	Bi content /wt%	Surface area/m^2/g	Pore volume/cm^3/g	Pore diameter/nm
MCM-41	–	–	1095	1.24	4.5
CuO/Bi_2O_3	69.4	7.9	27	0.08	6.8
CuO/Bi_2O_3/MCM-41	23.0	6.1	709[a]	0.76[b]	4.4
MK catalyst	35.6	4.0	45	0.08	4.4

[a]MCM-41 surface area in CuO/Bi_2O_3/MCM-41 samples.
[b]MCM-41 pore volume in CuO/Bi_2O_3/MCM-41 samples.

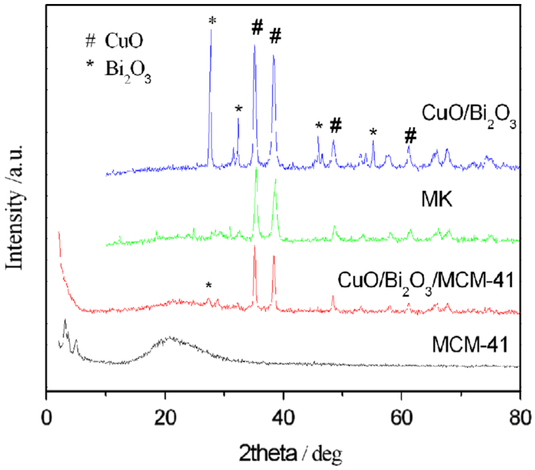

Fig. 1. XRD patterns of MCM-41 and catalyst samples.

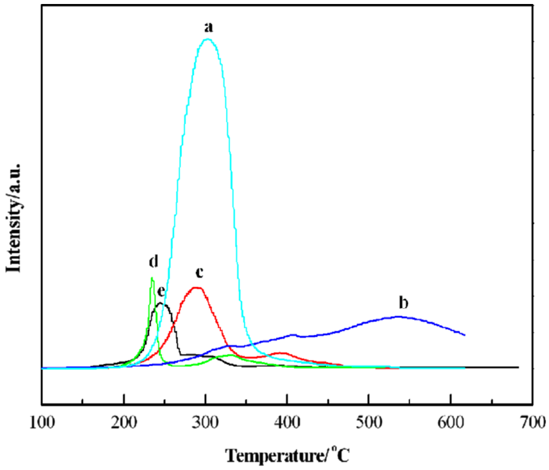

Fig. 2. H_2-TPR profiles of samples with the same weight ((a) CuO; (b) Bi_2O_3; (c) CuO/Bi_2O_3; (d) CuO/Bi_2O_3/MCM-41; (e) MK).

with CuO/Bi_2O_3 and MK catalysts, the CuO and Bi_2O_3 species probably dispersed better on MCM-41 material due to its large surface area and pore volume.

3.2. XRD

The XRD patterns of the three catalysts and MCM-41 zeolite are shown in Fig. 1. The diffraction peaks of the blank MCM-41 was typical peaks of the highly-ordered mesoporous MCM-41 material [22]. After the impregnation of $Cu(NO_3)_2$ and $Bi(NO_3)_3$ solutions and calcination, the order of the MCM-41 zeolite structure was decreased, although the main structure of MCM-41 still remained as evidenced by the existence of the main (110) diffraction peak [23]. For the CuO/Bi_2O_3/MCM-41 catalyst, three other diffraction peaks were detected at 2 theta angles of 35.2°, 38.4° and 48.4°, which were all ascribed to those of bulk CuO species [24]. Despite the fact that the Cu content decreased from 69.4 wt% in the CuO/Bi_2O_3 catalyst to only 23 wt% in the CuO/Bi_2O_3/MCM-41 catalyst, the CuO diffraction peaks was still observed for the latter catalyst with the intensities weakening. This suggests that the same CuO crystal structure occurred in the CuO/Bi_2O_3/MCM-41 and CuO/Bi_2O_3 catalysts. The average CuO crystal size calculated from the Scherrer equation was 19 nm for CuO/Bi_2O_3/MCM-41 and 54 nm for CuO/Bi_2O_3. Different from the situation for the main CuO active phase, the typical diffraction peaks of α-Bi_2O_3 at 27.7°, 32.3°, 45.8° and 55.3° [25] were observed as strong peaks for unsupported CuO/Bi_2O_3 catalyst but were hardly observed for CuO/Bi_2O_3/MCM-41 catalyst. These observations suggest that the Bi species were present in a highly dispersed state on mesoporous MCM-41 zeolite [26], although the Bi content (7.9%) in CuO/Bi_2O_3 was similar to that (6.1%) in CuO/Bi_2O_3/MCM-41 catalyst.

The XRD patterns of commercial Cu/Bi-based MK catalyst were similar to that of CuO/Bi_2O_3/MCM-41 catalyst except for the diffraction peaks of their carriers. The diffraction peak intensities of CuO species on commercial MK catalyst were slightly stronger than those on CuO/Bi_2O_3/MCM-41 catalyst. The average CuO crystal size calculated from the Scherrer equation was 13 nm for the MK catalyst. The crystallite size of CuO was found to follow the order CuO/Bi_2O_3 catalyst > CuO/Bi_2O_3/MCM-41 catalyst > MK catalyst.

3.3. H_2-TPR

The H_2-TPR profiles of CuO, Bi_2O_3, CuO/Bi_2O_3, CuO/Bi_2O_3/MCM-41 and MK samples are shown in Fig. 2. For pure CuO, a main H_2 consumption peak was observed around 310 °C, which was attributed to the reduction of bulk CuO [27]; while for pure Bi_2O_3, three H_2 consumption peaks with relatively high temperatures were generated in the range of 215–625 °C [25]. The H_2-TPR profile of Bi_2O_3 trailed off at high temperatures, indicating that the pure Bi_2O_3 compound was not easily reduced by H_2 [28]. The reduction peak of CuO in the CuO/Bi_2O_3 catalyst was slightly shifted to low temperature, i.e. 295 °C, suggesting that the addition of Bi_2O_3 was beneficial to the dispersion of CuO and its reduction [29]. This conclusion could be further illustrated by the H_2-TPR profile of CuO/Bi_2O_3/MCM-41, in which the reduction peak temperature of CuO was clearly decreased to 235°C owing to the relatively high dispersion of CuO on the large surface area MCM-41 zeolite or Cu^{2+} ions in an octahedral environment [30]. For the H_2-TPR profile of commercial MK catalyst, the reduction peak temperature of CuO was 246 °C, this being higher slightly than that of CuO in CuO/Bi_2O_3/MCM-41 catalyst; this indicates that CuO was dispersed better on MCM-41 than in MK catalyst.

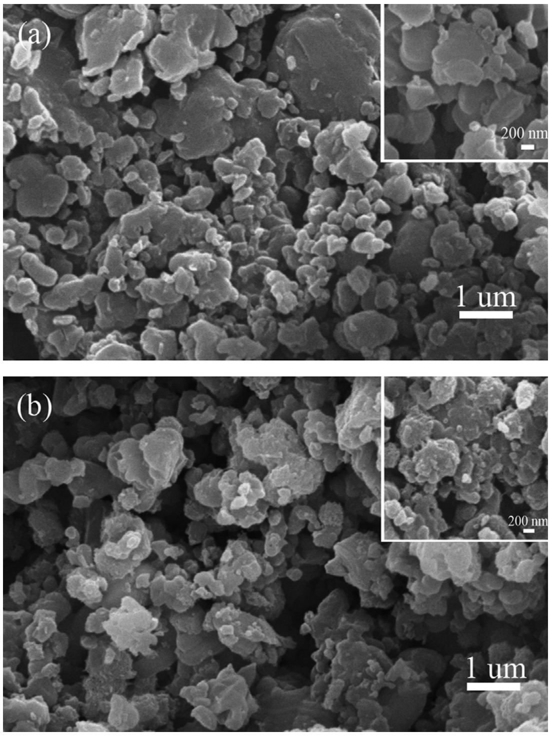

Fig. 3. SEM images of the blank MCM-41 sample (a) and the CuO/Bi_2O_3/MCM-41sample (b).

3.4. SEM

The SEM images of the blank MCM-41 and CuO/Bi_2O_3/MCM-41 samples are shown in Fig. 3. It could be seen from Fig. 3a that the surface of the blank MCM-41 was smooth. However, from Fig. 3b the surface of the MCM-41 loaded CuO and Bi_2O_3 showed rough. This implied CuO and Bi_2O_3 were located as small particles on the irregular MCM-41 [31]. The size of CuO particles was about over 10 nm, which was consistent with XRD results.

3.5. Catalytic activity for the ethynylation of formaldehyde

The catalytic activities of the prepared catalysts and the MK catalyst for the ethynylation of formaldehyde are listed in Table 2. It was found that the blank MCM-41 had no catalytic activity for the ethynylation reaction of formaldehyde, while other catalysts containing CuO and Bi_2O_3 showed catalytic activity. This meant that CuO and/or Bi_2O_3 were an essential active. Due to the different CuO loadings in the catalysts above, the amount of catalyst used in the catalytic runs was normalized to a fixed amount of CuO. It can be seen from Table 2 that CuO supported on the MCM-41 improved catalytic activity: the HCHO conversion increased from 29% for CuO/Bi_2O_3 catalyst to 51% for CuO/Bi_2O_3/MCM-41 catalyst. Also, more importantly, 1,4-butynediol selectivity increased from 70% to 93.7%. Although the same weight of CuO catalyst was used, CuO/Bi_2O_3 catalyst and CuO/Bi_2O_3/MCM-41 catalyst exhibited a difference in catalytic activity because MCM-41, with its large surface area and ordered mesopore structures, yielded a high dispersion of CuO (See Fig. 2 H_2-TPR) and Bi_2O_3 (See Fig. 1 XRD); hence, more active sites were obtained, which gave the higher HCHO conversion and 1,4-butynediol selectivity.

Compared with the commercial MK catalyst, now applied in a Chemical company in China and which gave just 37% HCHO conversion and 71% selectivity to 1,4-butynediol, CuO/Bi_2O_3/MCM-41 catalyst gave better conversion and selectivity under the same conditions (line 4 in Table 2). Considering MK catalyst with 45 m^2/g surface areas and 0.08 cm^3/g pore volume (line 4 in Table 1), we could speculate that the MK catalyst was small surface area and pore volume resulting in CuO congregation and lower catalytic activity. Apparently, MCM-41 allowed better dispersion of CuO and

Table 2
Activity of different catalysts in ethynylation reaction.[a]

Catalyst	Cu content/wt%	Catalyst quantities/g	HCHO conversion/%	1,4-butynediol selectivity/%
MCM-41	0	1.2	0	0
CuO/Bi_2O_3	69.4	0.4[b]	29.0	70.0
CuO/Bi_2O_3/MCM-41	23.0	1.2	51.1	93.7
MK catalyst	35.6	0.8[c]	37.0	71.0

[a] Reaction conditions: reaction temperature 90 °C, reaction time 7 h, reaction pressure: atmospheric pressure, pH value 7.5, Formeldehyde volume: 20 g (20 wt%).
[b] The same weight of Cu as that for the CuO/Bi_2O_3/MCM-41.
[c] The same weight of Cu as that for the CuO/Bi_2O_3/MCM-41.

Bi_2O_3 and CuO/Bi_2O_3/MCM-41 catalyst showed superior activity for 1,4-butynediol synthesis than the commercial MK catalyst and the unsupported CuO/Bi_2O_3 catalyst.

4. Conclusions

MCM-41 supported CuO/Bi_2O_3 nanoparticles catalyst was successfully prepared by a facile impregnation method. Compared with unsupported CuO/Bi_2O_3 and commercial Cu/Bi-based catalyst, CuO/Bi_2O_3/MCM-41 catalyst showed a superior catalytic activity toward the ethynylation reaction of formaldehyde for 1,4-butynediol synthesis. The results demonstrate that the CuO/Bi_2O_3/MCM-41 catalyst has excellent potential applications for fabrication high performance catalyst for 1,4-butynediol synthesis in industrial areas.

Acknowledgments

The authors thank Scientific Research Programmes of Colleges in Xinjiang (XJEDU2010S02) and Key Laboratory of Oil & Gas Fine Chemicals, Ministry of Education and Xinjiang Uyghur Autonomous Region, Xinjiang University (XJDX0908-2009-06) for financial supports.

References

[1] S. Tanielyan, S. Schmidt, N. Marin, G. Alvez, R. Augustine, Selective hydrogenation of 2-butyne-1,4-diol to 1,4-butanediol over particulate raney nickel Catalysts, Topics in Catalysis 53 (2010) 1145–1149.

[2] K. Kriaa, J.P. Serin, F. Contamine, P. Cézac, J. Mercadier, 2-Butyne-1,4-diol hydrogenation in supercritical CO_2: effect of hydrogen concentration, Journal of Supercritical Fluids 49 (2009) 227–232.

[3] J.M. Nadgeri, M.M. Telkar, C.V. Rode, Hydrogenation activity and selectivity behavior of supported palladium nanoparticles, Catalysis Communications 9 (2008) 441–446.

[4] H.T. Li, Y.X. Zhao, C.G. Gao, Y.Z. Wang, Z.J. Sun, X.Y. Liang, Study on deactivation of Ni/Al_2O_3 catalyst for liquid phase hydrogenation of crude 1,4-butanediol aqueous solution, Chemical Engineering Journal 181/182 (2012) 501–507.

[5] K.Hari Prasad Reddy, N. Anand, P.S. Sai Prasad, K.S. Rama Rao, B. David Raju, Influence of method of preparation of Co–Cu/MgO catalyst on dehydrogenation/dehydration reaction pathway of 1,4-butanediol, Catalysis Communications 12 (2011) 866–869.

[6] P. Luo, W.B. Wu, Y.H. Li, X.B. Zhang, X.W. Lv, X.D. Li, Support-containing catalyst for production of 1,4-butynediol by Reppe method, preparation method and application thereof, CN 102125856 A, 2011.

[7] R. Pinkos, R. E. Lorenz, Y. A. Beste, Process for preparing 1,4-butanediol, US 7759531 B2, 2010.

[8] T. Haas, B. Jaeger, R. Weber, S.F. Mitchell, C.F. King, New diol processes: 1,3-propanediol and 1,4-butanediol, Applied Catalysis A 280 (2005) 83–88.

[9] I.T. Duncanson, I.W. Sutherland, B. Cullen, S.D. Jackson, D. Lennon, The hydrogenation of 2-butyne-1,4-diol over a carbon-supported palladium catalyst, Catalysis Letter 103 (2005) 195–199.

[10] M.M. Telkar, C.V. Rode, R. Jaganathan, V.H. Rane, R.V. Chaudhari, Platinum catalyzed hydrogenation of 2-butyne-1,4-diol, Journal of Molecular Catalysis 187 (2002) 81–93.

[11] W. Zhang, R.H. Wang, Nonsupported catalysts for producing 1,4-butynediol and their preparation and application, CN 1118342A, 1996.

[12] J.Y. Wang, Y. Jiang, J.C. Xie, J.H. Chen, X.X. Zhang, W. Jiang, The research on preparation of butynediol using self-made malachite, Hecheng Huaxue (China) 18 (suppl) (2010) 26–29.

[13] Y.M. Gao, H.S. Tian, Y.F. Zhu, Catalytic synthesis on 1,4-butynediol by CuO/Bi_2O_3 particles, Guangdong Huagong (China) 35 (9) (2008) 53–55.

[14] Y. Zheng, Z.J. Sun, Y.Z. Wang, H.T. Li, S.A. Wang, M. Luo, J.L. Zhao, Y.X. Zhao, Preparation of $CuO–Bi_2O_3$ /SiO_2–MgO catalyst and its ethynylation performance, Fenzi Cuihua (China) 26 (3) (2012) 233–238.

[15] M.X. Yang, X.F. Zhang, Q.F. Huang, S. Lin, Study on preparation of CuO/Bi_2O_3/ZSM-5 catalyst and catalytic properties for synthesis of butynediol, Fenzi Cuihua (China) 21 (1) (2007) 58–60.

[16] P. Luo, X.M. Zhao, H.X. Li, H. Zhao, Y.H. Li, X.W. Lv, X.D. Li, Research of EQ-201 acetylene catalyst in reppe synthesizing 1,4-butynediol, Chemical Engineering Design Communications 38 (2012) 87–90.

[17] L. Zhong, M.Y. Zhao, S.J. Lv, F.L. Qiu, The study of the ethynylation catalyst for the butynediol, Natural Gas Huagong (China) 6 (1989) 5–8.

[18] D.S. Zhang, R.J. Wang, X.X. Yang, Beckmann rearrangement of cyclohexanone oxime over Al-MCM-41 and P modified Al-MCM-41 molecular sieves, Catalysis Communications 12 (2011) 399–402.

[19] A. Jha, A.C. Garade, S.P. Mirajkar, C.V. Rode, MCM-41 supported phosphotungstic acid for the hydroxyalkylation of phenol to phenolphthalein, Industrial & Engineering Chemistry Research 51 (2012) 3916–3922.

[20] V. Ambrogi, L. Latterini, F. Marmottini, C. Pagano, M. Ricci, Mesoporous silicate MCM-41 as a particulate carrier for octyl, Journal of Pharmaceutical Sciences 102 (2013) 1468–1475.

[21] R. Janus, A. Wach, P. Kust rowski, B. Dudek, M. Drozdek, M Investigation on the low-temperature transformations of poly (furfuryl alcohol) deposited on MCM-41, Langmiur 29 (2013) 3045–3053.

[22] L. Ma, J.B. Ji, F.W. Yu, N. Ai, H.T. Jiang, Post-synthesis of TiO_2/MCM-41 from aqueous $TiCl_4$ solution: structure, characteristics and epoxy catalytic activity, Microporous and Mesoporous Materials 165 (2013) 6–13.

[23] B.P. Ajayi, B. Rabindran Jermy, K.E. Ogunronbi, B.A. Abussaud, S. Al-Khattaf, n-Butane dehydrogenation over mono and bimetallic MCM-41 catalysts under oxygen free atmosphere, Catalysis Today 204 (2013) 189–196.

[24] A. Patel, P. Shukla, T. Rufford, S.B. Wang, J.L. Chen, V. Rudolph, Z.H. Zhu, Catalytic reduction of NO by CO over copper-oxide supported mesoporous silica, Applied Catalysis A 409/410 (2011) 55–65.

[25] X.J. Liu, L.k. Pan, J.L. Li, K. Yu, Z. Sun, Visible light-induced photocatalytic activity of Bi_2O_3 prepared via microwave-assisted method, Journal of Nanoscience and Nanotechnology 13 (2013) 5044–5047.

[26] X.L. Tang, X. Meng, L. Shi, Desulfurization of model gasoline on modified bentonite, Industrial & Engineering Chemistry Research 50 (2011) 7527–7533.

[27] G. Aguila, S. Guerrero, P. Araya, Effect of the preparation method and calcination temperature on the oxidation activity of CO at low temperature on $CuO–CeO_2/SiO_2$ catalysts, Applied Catalysis A 462/ (463) (2013) 56–63.

[28] Y. Lou, L. Wang, Y.H. Zhang, Z.Y. Zhao, Z.G. Zhang, G.Z. Lu, Y. Guo, The effects of Bi_2O_3 on the CO oxidation over Co_3O_4, Catalysis Today 175 (2011) 610–614.

[29] J. Li, P.F. Zhu, S.F. Zuo, Q.Q. Huang, R.X. Zhou, Influence of Mn doping on the performance of $CuO–CeO_2$ catalysts for selective oxidation of CO in hydrogen-rich streams, Applied Catalysis A 381 (2010) 261–266.

[30] G. Saidulu, N. Anand, K.S.R. Rao, A. Burri, S.E. Park, D.R. Burri, Cu/SBA-15 is an efficient solvent-free and acid-free catalyst for the rearrangement of benzaldoxime into benzamide, Catalysis Letter 141 (2011) 1865–1871.

[31] F. Soofivand, M. Salavati-Niasari, Novel solvent-less synthesis of CuO nanoparticles by using sublimated precursors, Materials Letters 106 (2013) 83–86.